Application of photon correlation spectroscopy to flowing Brownian motion systems

D. P. Chowdhury, C. M. Sorensen, T. W. Taylor, J. F. Merklin, and T. W. Lester

In this paper we study the application of photon correlation spectroscopy to a system of randomly diffusing particles suspended in a fluid undergoing uniform translational motion relative to the optical scattering volume. To do so we derive theoretical expressions for both the homodyne and heterodyne correlation functions in both the dilute and nondilute particle limits. We then test these results with experiments on a flowing system and find good agreement. We discuss a useful method of analysis and define limits to particle sizing in such a system using this light-scattering technique.

I. Introduction

Flowing Brownian motion systems of particles are encountered in a number of practical situations of interest including the study of soot particles in flames[1,2] and various aerosols.[3] Recently the dynamic light-scattering technique photon correlation spectroscopy (PCS) proved useful for studying diffusional processes in these aerosol systems as well as particle sizing. Thus it has become important that the theory of PCS for such a system be discussed in a manner amenable for use in these experiments and tested against an idealized experiment to facilitate its use. In this paper we shall recount the theoretical derivation of the PCS spectrum for a system of flowing Brownian motion particles and compare the results to a representative system of a suspension of polystyrene latex spheres in water flowing through a tube at known flow rate. This system is quite simple and will allow for verification of the theoretical spectrum and establish an experimental basis for the more complicated systems of interest.

In Sec. II we will outline the major steps in the derivation of the PCS spectrum for a flowing Brownian motion system relying, in large part, on the results of earlier workers.[4] Section III will describe a useful method of data analysis using a graphical display. Section IV will describe our experiment on the flowing aqueous suspension, Sec. V will compare the experimental measurements to theory and discuss the limits of measurement of key parameters. A summary is given in Sec. VI.

II. Theory

In this section we wish to display the principal ingredients leading to the intensity autocorrelation function of the light scattered from a system of particles undergoing random Brownian diffusional motion and uniform translation relative to the scattering volume. The complete development for the heterodyne detection mode can be found in the article by Edwards *et al.*[4] for the power spectrum of the scattered light, the Fourier transform of the intensity autocorrelation function. In this paper we will present both the heterodyne and homodyne correlation functions with emphasis on the homodyne function which, while being somewhat more complex, is the most straightforward to set up experimentally. Our method is similar to Edwards *et al.*, although we have incorporated certain elements of the book by Berne and Pecora[5] which may also be used as a source for the outline we shall present.

We begin by describing $E_s(t)$, the complex scalar scattered-light electric field. We shall only consider the light scattered with polarization parallel to the incident field and perpendicular to the scattering plane defined by the incident and scattered wave vectors $\mathbf{K}_{\text{inc}}$ and $\mathbf{K}_{\text{scat}}$. For $E_s(t)$ one has

$$E_s(t) = \sum_{j=1}^{N_T} \exp(i\mathbf{q} \cdot \mathbf{r}_j) P(\mathbf{r}_j). \tag{1}$$

Here $\mathbf{q} = \mathbf{K}_{\text{inc}} - \mathbf{K}_{\text{scat}}$ is the scattering wave vector which, for quasi-elastic scattering, has magnitude

$$q = \frac{4\pi n}{\lambda} \sin\theta/2, \tag{2}$$

T. W. Lester is with Louisiana State University, Department of Mechanical Engineering, Baton Rouge, Louisiana 70803; the other authors are with Kansas State University, Departments of Nuclear Engineering & Physics, Manhattan, Kansas 66506.

Received 21 May 1984.
0003-6935/84/224149-06$02.00/0.

where λ, n, and θ are the wavelength, medium refractive index, and scattering angle, respectively. The sum in Eq. (1) is carried out over all the particles in the system with positions $\mathbf{r}_j$. An amplitude function $P(\mathbf{r}_j)$ describes the incident light amplitude as a function of $\mathbf{r}$. For an incident laser beam operating in the typical TEM_{00} mode, $P(\mathbf{r})$ would be described by a cylindrically symmetric Gaussian profile. For our purposes one may approximate $P(\mathbf{r})$ as a spherically symmetric Gaussian

$$P(\mathbf{r}) = E_0 \exp(-r^2/w^2), \tag{3}$$

where w is the beam waist. This is not an unreasonable approximation because the view of the incident Gaussian beam will most likely be vignetted somewhat on its way to the detector. Furthermore, it is the Gaussian nature of the beam perpendicular to the scattering plane which affects our results, not the assumed Gaussian nature parallel to this plane.

For our particular system the position vector $\mathbf{r}_j$ may be decomposed into two independent, translational and diffusional, parts:

$$\mathbf{r}_j(t) = \mathbf{v}t + \mathbf{r}_j'(t). \tag{4}$$

In Eq. (4) $\mathbf{v}$ is the flow velocity, and $\mathbf{r}_j'(t)$ is due solely to the diffusion. Equations (1)–(4) present a description of the scattered light field for the translation-diffusion system.

The scattered light may be detected in either of two ways: heterodyne detection, where the scattered light is coherently mixed on the photomultiplier cathode with a more intense portion of the original incident beam which acts as a local oscillator; and homodyne detection, where the scattered light coherently mixed with itself. Thus two intensity autocorrelation functions are needed to describe these two detection modes. Following Berne and Pecora, we define

$$I_1(t) \equiv \langle E_s(t)E_s^*(0)\rangle, \tag{5a}$$

$$I_2(t) \equiv \langle |E_s(t)|^2 |E_s(0)|^2\rangle. \tag{5b}$$

The brackets indicate an ensemble average to be described below, and the asterisk designates complex conjugation.

Under the assumption of independent or uncorrelated scattering particles, the heterodyne and homodyne scattered-light autocorrelation functions are[5]

$$\langle I(t)I(0)\rangle_{\text{het}} = [I_{\text{lo}}^2 + 2I_{\text{lo}}\,\text{Re}I_1(t)], \tag{6a}$$

$$\langle I(t)I(0)\rangle_{\text{hom}} = I_2(t). \tag{6b}$$

In Eqs. (6), I_{lo} is the intensity of the local oscillator light, and Re means real part. Thus the problem for obtaining the experimentally measured Eqs. (6) becomes one of evaluating Eqs. (5) for the scattered light described by Eqs. (1)–(4).

To calculate the autocorrelation functions I_1 and I_2 we must recognize that the average implied by the brackets is, in fact, two averages; one over the diffusional motion of the particle, and the other over the translational motion which is effected by averaging over the initial position of the particles with respect to $P(\mathbf{r})$. Furthermore, we shall assume that the diffusive displacement for times comparable with the experimental correlation time is much less than the characteristic size w of the scattering volume. Then these two averages may be taken as independent and thus separable.

Proceeding with the calculation of I_1 we write, from Eqs. (1) and (5a),

$$I_1 = \exp(i\mathbf{q}\cdot\mathbf{v}t)\sum_{j,k}\langle\exp[i\mathbf{q}\cdot\delta\mathbf{r}_{j,k}(t)]\rangle_{\delta\mathbf{r}} \times \langle P[\mathbf{r}_j(0)]P[\mathbf{r}_k'(t)+\mathbf{v}t]\rangle_{\mathbf{r}(0)}. \tag{7}$$

Here $\delta\mathbf{r}_{j,k}(t) = \mathbf{r}_j'(t) - \mathbf{r}_k'(0)$, and the averages have been separated into the diffusional, $\langle\ldots\rangle_{\delta\mathbf{r}}$, and initial position, $\langle\ldots\rangle_{\mathbf{r}(0)}$, terms. For a system of noninteracting particles, these averages are zero for $j \neq k$ due to particle independence. Thus only $j = k$ terms survive. The diffusional average is well known[4–6] and is found by integrating over the normalized Gaussian probability distribution, the solution to the diffusion equation. Thus

$$\langle\exp[i\mathbf{q}\cdot\delta\mathbf{r}(t)]\rangle = \exp(-Dq^2t), \tag{8}$$

where D is the diffusion coefficient.

To calculate the positional average we integrate over the probability of finding the jth particle initially in a volume element d^3r. If V_T is the total volume of the system, this probability is $V_T^{-1}d^3r$. Using Eq. (3) the second average in Eq. (7) is

$$E_0^2V_T^{-1}\int d^3r\exp\left(-\frac{r^2}{w^2}\right)\exp\left[-\frac{(\mathbf{r}+\mathbf{v}t)^2}{w^2}\right] = E_0^2V_T^{-1}\left(\frac{\pi}{2}\right)^{3/2}\times w^3\exp(-v^2t^2/2w^2). \tag{9}$$

An effective scattering volume can be determined by integrating the Gaussian intensity function $P^2(r)$ over all space. One finds $V_s = (\pi/2)^{3/2}w^3$; then

$$\langle PP(t)\rangle_{\mathbf{r}(0)} = E_0^2V_sV_T^{-1}\exp(-v^2t^2/2w^2). \tag{10}$$

Finally, summing over j we find

$$I_1(t) = I_0\langle N\rangle\exp(i\mathbf{q}\cdot\mathbf{v}t)\exp(-Dq^2t)\exp(-v^2t^2/2w^2), \tag{11}$$

where $I_0 = E_0^2$ and $\langle N\rangle = N_TV_sV_T^{-1}$ is the average number of particles in V_s. This may be substituted into Eq. (6) to obtain the heterodyne correlation function.

Equation (11) shows that the heterodyne correlation function is a product of three terms. The first term is a sinusoidal Doppler shift term due to the translational flow of the particles. The second is an exponential decay due to the diffusional motion, and the third is Gaussian in time dependent on the transit time w/v of the particles through the incident laser beam due to the flow.

The calculation of I_2 is somewhat more complex. Substitution of Eq. (1) into Eq. (5b) yields an expression involving a sum over four particle indices, j, k, l, and m:

$$I_2(t) = \Big\langle \sum_{j,k,l,m} \exp[i\mathbf{q}\cdot\mathbf{r}_j(0)]P[\mathbf{r}_j(0)] \times \exp[-i\mathbf{q}\cdot\mathbf{r}_k(0)]P[\mathbf{r}_k(0)] \times \exp(i\mathbf{q}\cdot\mathbf{v}t)\exp[i\mathbf{q}\cdot\mathbf{r}_l(t)]P[\mathbf{r}_l(t)+\mathbf{v}t] \times \exp(-i\mathbf{q}\cdot\mathbf{v}t)\exp[-i\mathbf{q}\cdot\mathbf{r}_m(t)]P[\mathbf{r}_m(t)+\mathbf{v}t]\Big\rangle . \quad (12)$$

Particle independence, however, will cause the ensemble average to be zero if any one of these four indices is distinct. Consequently, only two kinds of term survive, those for which (a) $j = k$ and $l = m$ including $j = k = l = m$, and (b) $j = m$, $k = l$, $j \neq k$.

For case (a),

$$I_{2,a}(t) = \Big\langle \Big\langle \sum_{j,l} P^2[\mathbf{r}_j(0)]P^2[\mathbf{r}_l(t)+\mathbf{v}t] \Big\rangle_{\mathbf{r}(0)} \Big\rangle_{\delta\mathbf{r}}. \quad (13)$$

Once again we assume $\delta\mathbf{r} \ll \mathbf{v}t$. Then the diffusional average has no consequence. The initial position average is found as above by integrating over $V_T^{-1}d^3r$. Thus for $j \neq l$,

$$I_{2,a}(t) = E_0^4 \sum_{j\neq l} V_T^{-2} \iint d^3r_j d^3r_l \exp\left(\frac{-2r_j^2}{w^2}\right)\exp\left[\frac{-2(\mathbf{r}_l+\mathbf{v}t)^2}{w^2}\right] = I_0^2\langle N(N-1)\rangle. \quad (14)$$

Here as above we used $V_s = (\pi/2)^{3/2}w^3$, $I_0 = E_0^2$ and the fact that the average number of terms in the sum times $(V_s/V_T)^2$ is $\langle N(N-1)\rangle$, where N is the number of particles in the scattering volume.

The $j = k = l = m$ term is found by evaluating

$$I'_{2,a}(t) = E_0^4 \sum_j V_T^{-1} \int d^3r_j \exp\left(-\frac{2r_j^2}{w^2}\right)\exp\left[-\frac{2(\mathbf{r}_j+\mathbf{v}t)^2}{w^2}\right] = E_0^4 N_T V_T^{-1}\exp\left(-\frac{v^2t^2}{w^2}\right)2^{-3/2}(\pi/2)^{3/2}w^3 = I_0^2\langle N\rangle 2^{-3/2}\exp\left(-\frac{v^2t^2}{w^2}\right). \quad (15)$$

For case (b) using $\delta\mathbf{r}(t) \ll \mathbf{v}t$ and independence of averages over $\delta\mathbf{r}$ and $\mathbf{r}(0)$,

$$I_{2,b}(t) = \sum_{j\neq l} \langle P[\mathbf{r}_j(0)]P[\mathbf{r}_j(t)+\mathbf{v}t] \times P[\mathbf{r}_l(0)P[r_l(t)+\mathbf{v}t]\rangle_{\mathbf{r}(0)} \times \langle \exp(i\mathbf{q}\cdot\delta\mathbf{r}_{j,m})\exp(i\mathbf{q}\cdot\delta\mathbf{r}_{l,k})\rangle_{\delta\mathbf{r}}. \quad (16)$$

Independence of particles yields

$$I_{2,b}(t) = \sum_{j\neq l} \langle PP(t)\rangle^2 \,|\langle\exp(i\mathbf{q}\cdot\delta\mathbf{r})\rangle|^2 = I_0^2\langle N(N-1)\rangle\exp\left(-\frac{v^2t^2}{w^2}\right)\exp(-2Dq^2t). \quad (17)$$

The last line follows from results above. Following Berne and Pecora, the number of particles in the scattering volume should follow a Poisson distribution for which $\langle N(N-1)\rangle = \langle N\rangle^2$. We can now combine terms to write $I_2(t)$, the homodyne correlation function, as

$$I_2(t) = \langle N\rangle^2\left[1+\exp(-2Dq^2t)\exp\left(-\frac{v^2t^2}{w^2}\right)\right] + 2^{-3/2}\langle N\rangle\exp\left(-\frac{v^2t^2}{w^2}\right). \quad (18)$$

The last term in Eq. (18) is often called the non-Gaussian term (although it is Gaussian in time) because it would not be present if there were a sufficient number of scatterers to ensure Gaussian statistics for the scattered light. In the Gaussian limit, $I_1(t)$ and $I_2(t)$ are simply related by the Siegart relation

$$I_2(t) = \langle N\rangle^2 I_0^2 + |I_1(t)|^2. \quad (19)$$

Since the non-Gaussian term is only linearly dependent on $\langle N\rangle$, it becomes relatively small for $\langle N\rangle \gtrsim 100$, the nondilute limit. This limit may not always be obtained, however, for some systems, especially aerosols, which are characteristically less dense than liquid phase suspensions.

Our result for the coefficient of the non-Gaussian term contains a factor of $2^{-3/2}$, which we have not found in earlier literature. This factor is a result of the fact that the effective volume as we have defined it of a spherical Gaussian scattering volume decreases by $2^{-3/2}$ when the Gaussian function is squared. Berne and Pecora, whose methods we have largely followed, do not obtain this factor. They used a step function beam profile, however, whose effective volume does not change when the step function is squared. Thus, the factor is dependent on our assumption of a spherically symmetric scattering volume and may vary somewhat for a real system.

The Gaussian term, proportional to $\langle N\rangle^2$, in Eq. (18) again shows a product of two competing signals: the exponential due to the particle diffusional motion, and the Gaussian in the time term due to the beam transit of the particles with flow velocity v. Quite often one wants to measure the exponential term because it contains size information. The second beam transit term can interfere with this measurement. In what follows we will explore the interplay between these two terms experimentally.

III. Data Analysis

In the nondilute limit, where $\langle N\rangle^{-1} \ll 1$, the experimental homodyne correlation function may be written as

$$\langle II(n\Delta t)\rangle = B + C(0)\exp\left[-\frac{n\Delta t}{\tau_1} - \frac{(n\Delta t_2)^2}{\tau_2^2}\right]. \quad (20)$$

Here B is an experimental background term, the signal to background, $C(0)/B$, being determined by extraneous light and coherence on the detector cathode. Time is measured digitally as $t = n\Delta t$, where n is a non-negative integer, and Δt is the sample time set on the digital correlator. The times $\tau_1 = (2Dq^2)^{-1}$ and $\tau_2 = w/v$ are, respectively, the correlation time containing the diffusional information and the beam transit time equal to the passage time of the particle through the laser beam due to the flow velocity and are the key experimental parameters.

To analyze the PCS spectrum the background term may be determined in any of the usual methods such as a preset delay to long times or calculated directly from count rate parameters. If we subtract B from Eq. (20), divide by $C(0)$, take the logarithm, and divide by $-n\Delta t$, we obtain

$$Y(n\Delta t) = -\frac{1}{n\Delta t}\ln\frac{C(n\Delta t)}{C(0)} = \frac{1}{\tau_1} + \left(\frac{1}{\tau_2}\right)^2 n\Delta t. \quad (21)$$

A plot of $Y(n\Delta t)$ vs $n\Delta t$ will be yield a straight line with slope equal to the inverse beam transit time squared and intercept equal to the inverse correlation time.

This method of analysis is not new and is, in fact, implicit in any application of the linear least-squares equation to an exponential such as Eq. (20). We have, however, found it very useful to graph Eq. (21) during analysis to indicate the presence of spurious signals that might go unnoticed during a computer fit. In this way we have detected the presence of both multiple scattering and photomultiplier afterpulsing in our signals as an anomalous upswing of $Y(n\Delta t)$ for small n. This can be understood since both multiple scattering and afterpulsing add correlation to the initial channels.

Equation (21) can be modified to ignore the first m channels and thus conveniently obviate the effects of such spurious signals in the early part of the spectrum. If we ignore the first $m-1$ channels, we may write from Eq. (20)

$$Y^m(n\Delta t) = -\frac{1}{(n-m)\Delta t}\ln\frac{C(n)}{C(m)} = \frac{1}{\tau_1} + \left(\frac{1}{\tau_2}\right)^2 (n+m)\Delta t. \quad (22)$$

This shows if we plot $Y^m(n\Delta t)$ vs $(n+m)\Delta t$ for $n > m$, the slope and intercept still yields τ_2 and τ_1, but problems in the first $m-1$ channels are eliminated.

IV. Experiment

A suspension of monodisperse polystyrene latex spheres in water has through the years provided a convenient and simple system with which to ensure the proper working of a PCS experiment. Here we again use this system only now providing a variable uniform flow rate to test the theoretical expression above and our data analysis method. Thus this simple system gives us a benchmark for future experiments on more complex situations such as soot particles in flames and aerosol systems.

Two 4-liter flasks acted as upper and lower reservoirs for our flow apparatus. The aqueous polystyrene suspension flowed out of the upper reservoir through a vertical precision bore glass tube 0.9525-cm i.d. and 1.78 m long, a flowmeter, a flow control valve, and then into the lower reservoir. Early experiments showed considerable nonlaminar or turbulence effects, which caused us to use the precision bore tube. The flow rate could be varied from 0 to 900 mliter/min yielding fluid velocities from 0 to 42 cm/sec and a maximum Reynolds number of 3800.

Suspension of two different sized particles was made: 0.091-μm diam with a concentration of 9.4×10^9 cm^{-3} and 0.234-μm diam with a concentration of 8.0×10^7 cm^{-3}. These concentrations were large enough to afford a strong signal yet low enough to ensure negligible multiple scattering.[7] These suspensions were made up in filtered distilled water, and the system was thoroughly cleaned and rinsed to eliminate contaminating particulates.

The light-scattering apparatus used an Ar-ion laser operating in the Gaussian TEM_{00} mode at $\lambda = 4880$ Å.

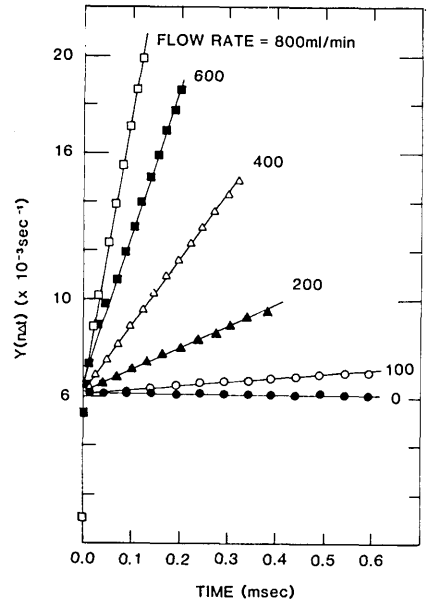

Fig. 1. Plot of $Y(n\Delta t)$ vs time $= n\Delta t$ for the 0.091-μm system at a variety of flow rates. Incident lens focal length was 30.0 cm.

The horizontal beam with vertical polarization was focused into the vertical flow tube with lenses of focal lengths ranging from 9.4 to 30.0 cm. Light scattered at 90° in the horizontal plane was collected by a lens and imaged onto an adjustable aperture which provided diffraction to give suitable coherence on an ITT FW 130 photomultiplier tube. The photopulses were amplified and discriminated and then passed to a commercial correlator which computed the homodyne correlation function. Data were analyzed with an on-line microcomputer.

V. Results

Zero flow rate measurements showed the proper q^2 dependence of the correlation time τ_1. The effects of finite flow rates are illustrated in Fig. 1, where the data are plotted in accordance with the slope-intercept method of Eq. (21). As can be seen, straight lines are obtained indicating the spectrum has the form of an exponential multiplied by a Gaussian in time as predicted in Eq. (18). Furthermore, except for a few points below the intercept due to dead-time effects in the detection electronics, the intercept remains fairly constant for various flow rates as expected since it should be only dependent on the diffusional motion of the particles.

Figure 2 displays a graph of the square root of the slope from Fig. 1 and two other incident lens configurations vs flow rate, which is proportional to v. Since the inverse of the square root of the slope of Fig. 1 is equal to the beam transit time τ_2, the straight line nature of Fig. 2 demonstrates that the beam transit time τ_2 is inversely proportional to v as predicted.

To test the dependence of τ_2 on the Gaussian beam waist w, we performed measurements with three different focal length lenses. The incident beam profile at the lens was measured and found to be Gaussian with

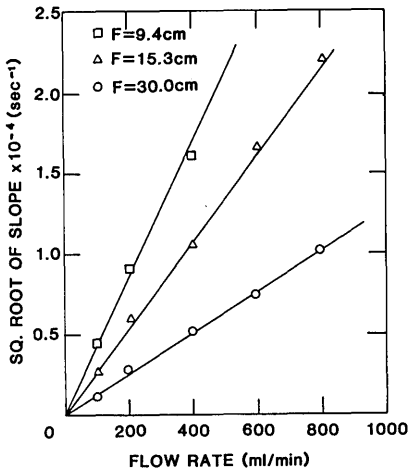

Fig. 2. Square root of the slope of the curves in Fig. 1 vs flow rate for $F = 30.0$ cm and two other incident lens focal lengths. The beam transit time τ_2 is the inverse of the square root of the slope.

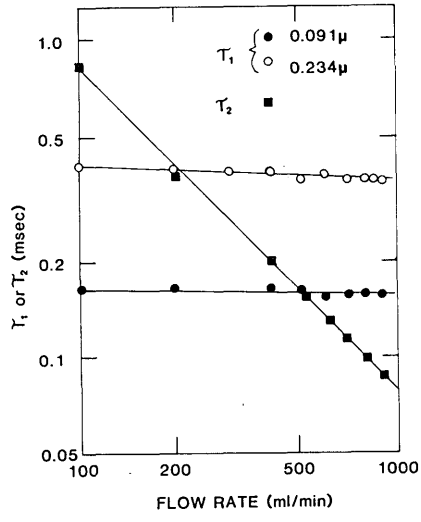

Fig. 3. Correlation time τ_1 or the beam transit time τ_2 vs flow rate for both sizes of microspheres. The flow velocity in the center of the tube is given by v(cm/sec) = $4.68 \times 10^{-2} \times$ flow rate (mliter/min).

waist $w_0 = 0.147$ cm. From Gaussian optics the focused beam waist is given by

$$w_1 = \frac{\lambda}{\pi w_0} f, \tag{23}$$

where f is the lens focal length. The beam does not focus at the focal distance but rather at a distance given by the standard geometric paraxial formula as if the light emanated from the center of the laser tube. This point was 4.5 m from our lens and thus caused the tightest focus to be at most a few centimeters beyond f from the lens. We adjusted the lens distance for the tightest focus.

The slopes of the three curves in Fig. 2 should be, by Eq. (18), related to the inverse of the focused beam waist w_1 in the flow tube. The curvature of the flow tube itself should not affect the focused waist in the vertical direction, which is the relevant direction since **v** is vertical. These slopes scale well with f and yield values of w_0 from Eq. (23) of 0.146, 0.153, and 0.139 cm for the f = 9.4-, 15.3-, and 30.0-cm lenses, respectively. These values are not only consistent with each other but agree very well with the measured incident beam waist.

We now consider the effect of flow on accurate determination of the correlation time τ_1, from which the particle diffusion coefficient and size can be determined. Figure 3 shows both τ_1 and τ_2 vs flow rate for the 0.091- and 0.234-μm suspensions. The correlation time should be independent of flow rate, and we see that this is nearly true even when the beam transit time is considerably faster, and hence the Gaussian term decays considerably quicker, than the correlation time. This result is quite pleasing since we had some concern regarding our ability to extract accurate correlation times, and hence particulate diffusion or size information, when $\tau_2 < \tau_1$. Some error still results, however, making τ_1 appear too small by as much as 30% for the largest flow rates when $\tau_2 \sim \frac{1}{5}\tau_1$.

Using the Stokes-Einstein diffusion constant

$$D = \frac{KT}{6\pi\eta r}, \tag{24}$$

where K is Boltzmann's constant, T is the temperature, and η is the shear viscosity, the particulate size r can be determined using $\tau_1 = (2Dq^2)^{-1}$. At zero flow rate we found the diameters from τ_1 to be 0.089 and 0.229 μm, which compare well with the nominal values of 0.091 and 0.234 μm given by the manufacturer. At the highest flow rate, when $\tau_2 < \tau_1$, the measured values were 0.086 and 0.164 μm. This latter size reflects the error incurred in a size measurement when $\tau_2 \sim \frac{1}{5}\tau_1$.

VI. Conclusion

We reformulated the theoretical expression for the intensity autocorrelation function of light scattered from a system of particles undergoing both random diffusional motion and uniform translation relative to the scattering volume. Our results are expressed in a form convenient for application to experiments on various systems including aerosol systems such as soot particles in a flame. The homodyne spectrum involves two terms: an exponential decay in time whose characteristic time is determined by the diffusional motion, and a Gaussian decay in time whose characteristic time is determined by the relative motion of the flowing system. For the nondilute limit these terms occur as a product in the correlation function.

We have tested the theory against a simple benchmark experiment involving a flowing suspension of polystyrene latex particles. Our graphical data analysis allowed for easy separation of the two terms and also acted as a diagnostic of, and enabled the removal of, spurious effects such as afterpulsing or multiple scattering. The results of the experiment agreed well with the theory and indicated that diffusional or size information contained in the correlation time could be extracted even when the beam transit time due to uniform flow was significantly faster.

We wish to thank G. B. King and S. M. Scrivner for help during the initial stages of this work. This work was supported by DOE grant DE-AC02-80ER10677 and NSF grant CPE-8218415.

References

1. G. B. King, C. M. Sorensen, T. W. Lester, and J. F. Merklin, "Photon Correlation Spectroscopy Used as a Particle Size Diagnostic in Sooting Flames," Appl. Opt. **21**, 976 (1982).
2. W. L. Flower, "Optical Measurements of Soot Formation in Premixed Flames," Combust. Sci. Technol. **33**, 17 (1983).
3. W. Hinds and P. C. Reist, "Aerosol Measurement by Laser Doppler Spectroscopy—I. Theory and Experimental Results for Aerosol Homogeneous," Aerosol Sci. **3**, 501 (1972).
4. R. V. Edwards, J. C. Angus, M. J. French, and J. W. Dunning, Jr., "Spectral Analysis of the Signal from the Laser Doppler Flowmeter: Time-Independent Systems," J. Appl. Phys. **42**, 837 (1972).
5. B. J. Berne and R. Pecora, *Dynamic Light Scattering* (Wiley, New York, 1976).
6. N. A. Clark, J. H. Lunacek, and G. B. Benedek, "A Study of Brownian Motion Using Light Scattering," Am. J. Phys. **38**, 575 (1970).
7. C. M. Sorensen, R. C. Mockler, and W. J. O'Sullivan, "Multiple Scattering from a System of Brownian Particles," Phys. Rev. **17**, 2030 (1978).

NATO Advanced Study Institute. "Laser Surface Treatment of Metals" San Miniato, Italy, 2-13 September 1985. For more information and application, write C. W. Draper, AT&T Technologies, P. O. Box 900, Princeton, NJ 08540 or P. Mazzoldi, Diparti di Fisica, Universita di Padova, 35131 Padova - via F. Marzolo, 8, Italy.